Theor Chem Acc (2001) 106:98–104
DOI 10.1007/s002140000214

Theoretical
Chemistry Accounts

Regular article

A computational model of the 5-HT_3 receptor extracellular domain: search for ligand binding sites

Maria Cristina Menziani[1], Francesca De Rienzo[1], Andrea Cappelli[2], Maurizio Anzini[3], Pier G. De Benedetti[1]

[1]Dipartimento di Chimica, Universita' di Modena e Reggio E., Via Campi 183, 41100 Modena, Italy
[2]Dipartimento Farmaco Chimico Tecnologico, Università di Siena, Via A. Moro, 53100 Siena, Italy
[3]Dipartimento di Scienze Farmaco-Biologiche, Università di Catanzaro "Magna Graecia", Complesso Ninì Barbieri, 88021 Roccelletta di Borgia, Catanzaro, Italy

Received: 27 July 2000 / Accepted: 15 September 2000 / Published online: 21 December 2000

Abstract. A three-dimensional model of the 5-HT_3 receptor extarcellular domain has been derived on the basis of the nicotinic acetylcholine receptor model recently published by Tsigelny et al. Maximum complementarity between the position and characteristics of mutated residues putatively involved in ligand interaction and the pharmacophoric elements derived by the indirect approach applied on several series of 5-HT_3 ligands have been exploited to gain insights into the ligand binding modalities and to speculate on the mechanistic role of the structural components. The analysis of the three-dimensional model allows one to distinguish among amino acids that exert key roles in ligand interactions, subunit architecture, receptor assembly and receptor dynamics. For some of these, alternative roles with respect to the ones hypothesized by experimentalists are assigned. Different binding modalities for agonists and antagonists are highlighted, and residues which probably play a role in the transduction of binding into a change in conformational state of the receptor are suggested.

Key words: Molecular modelling – 5-HT_3 receptor – Extracellular domain – Ligand binding site – Ligand-gated ion channel

1 Introduction

The 5-HT_3 receptor (5-HT_3R) is a member of the cysteine (Cys)-loop family of ligand-gated ion channels (LGICs), which includes the nicotinic acetylcholine receptor(nAChR), the γ-aminobutiric acid type A receptor ($GABA_A$R) and the glycine receptor (GlyR). These receptors play key roles in fast synaptic transmission through the nervous system. Agonist binding and channel gating occur at topographically distinct sites within the receptor molecule; therefore, a signal triggered by specific neurotransmitter molecules is converted into the opening of a cation-selective ion channel (5-HT_3R and nAChR) or an anion-selective ($GABA_A$R and GlyR) ion channel, via propagated conformational changes [1].

Despite the absence of X-ray crystallographic data, a three-dimensional image of the nAChR has emerged from electron microscopy data [2] and further information with respect to the agonist/antagonist binding sites, the ion channel and its selectivity filter have been derived by photoaffinity labelling and site-directed mutagenesis studies [3].

The high degree of homology of the Cys-loop receptors suggests that they might share common secondary, tertiary and quaternary structures. Moreover, experimental evidence for the same mechanism of coupling agonist binding to channel opening have been provided by a nAChR and a 5-HT_3R chimera [4].

Evidence for a rapid equilibrium among several functional states of the receptors (resting, active and desensitized) affected by reversibly binding ligands has been provided for the nAChR. In the resting state the receptor has low affinity for agonists and the channel is closed. Upon binding of agonists, the active state shows high probability for the channel opening. Finally, the desensitized state predominates after long agonist exposure; the affinity for agonists is the highest but the channel is closed. The resting and desensitized states are characterized by a different structure of the nAChR binding site [1].

The receptors are constituted by assemblies of five heterosubunits or homosubunits surrounding a central transbilayer pore. Each subunit has a large N-terminal extracellular domain, four putative transmembrane segments and an intracellular domain. Composite ligand binding sites, conserved throughout the Cys-loop receptor superfamily, are located at the interface of two subunits, formed by residues belonging to two components [5]. The transition to an open, active state of the

Correspondence to: M. C. Menziani
e-mail: menziani@unimo.it

Contribution to the Symposium Proceedings of Computational Biophysics 2000

nAChR seems to be favoured by the occupation of two agonist binding sites, but a ligand–receptor complex with a stoichiometry of 1:1 seems to be sufficient for the homomeric [6] 5-HT_3R function [7].

In parallel with the experimental approaches, efforts have been made to predict the secondary structure of the individual nAChR subunits with computational techniques [8, 9]. However, three-dimensional models of the extracellular domain have been derived, so far, only for the nAChR [10] and for the glycine receptor [11].

We have been involved for several years in the design, synthesis and pharmacological evaluation of 5-HT_3R ligands based on the arylpiperazine, quinuclidine and tropane structures [12, 13, 14] Extensive quantitative structure–affinity relationship studies carried out on the isolated ligands (indirect approach) resulted in a four-component pharmacophoric model shared by all the classes of compounds studied, involving

1. A charge-assisted hydrogen bond or an ionic interaction between the positively charged head of the ligand and a negatively charged carboxylic amino acid residue in the receptor.
2. A hydrogen-bonding interaction between a ligand acceptor atom (nitrogen or oxygen) and a hydrogen-bond donor in the receptor.
3. A specific interaction between an aromatic ring and a suitable amino acid residue in the receptor.
4. A zone in which short-range (e.g. van der Waals) interactions take place.

Since the series of ligands studied are constituted by both classical 5-HT_3R antagonists which contain the generally recognized pharmacophore (i.e. basic nitrogen, carbonyl group and aromatic ring) and atypical 5-HT_3R antagonists (a heterocyclic nitrogen atom replaces the carbonyl group) the interrelation between these different classes in the interaction with the receptor is far from obvious [12]. Moreover, peculiarities observed in the structure–affinity/activity relationships obtained for stereoselective ligands cannot be explained by an indirect approach applied on isolated ligands, although the main differences in their binding modes were somewhat taken into account in the supermolecule approach used in a recent study.

In fact, speculations on the details of the interaction mechanisms of stereoselective ligands can only be made on the receptor–ligand complexes (direct approach) obtained by performing suitable docking experiments on a working model of the central 5-HT_3R.

In this study, we derive a three-dimensional model of a 5-HT_3R extracellular domain fitting all the experimental information available to date on the nAChR model, recently published by Tsigenly et al. [10], which has been chosen as a template.

Maximum complementarity between the position and characteristics of mutated residues putatively involved in ligand interaction and the pharmacophoric elements derived by the indirect approach applied on several series of 5-HT_3 ligands have been exploited to gain insight into the ligand binding modalities and to speculate on the mechanistic role of the structural components.

2 Methods

2.1 Homology modelling

Sequences of the 5-HT_3R, the nAChR, the $GABA_A$R and GlyR were extracted from the EMBL protein sequence database and sequence alignment was achieved by means of the CLUSTALW program [15]. The atomic coordinates of the nicotinic receptor extracellular domain model, which we used as a template, were supplied by Taylor [10]. Homology modelling was performed using the program MODELLER [16]. The program deduces distance and angle constraints from the template structure and combines them with energetic terms for an adequate stereochemistry in an objective function which is later optimized in the Cartesian space with conjugate gradients and molecular dynamics (simulated annealing) methods. Fifteen conformations of the 5-HT_3R were generated through randomization of the Cartesian coordinates, with a deviation of ± 4 Å. The models obtained show appreciable differences only in the conformation of loop 130–140, which is the only region where deletion occurred with respect to the template structures.

2.2 Refinement and analysis of the three-dimensional structures

Energy minimization was performed for each of the fifteen models using the program CHARMM [17]. The minimization procedure consisted of 50 steps of steepest descent, followed by a conjugate gradient minimization until the root-mean-square gradient of the potential energy was less than 0.001 kcal/molÅ. The united atom force-field parameters, a 12-Å nonbonded cutoff and a dielectric constant $\varepsilon = 4r$ were used.

The choice of the best model obtained, among the ones generated by randomization of the Cartesian coordinates, was guided by

1. Evaluation of the overall fold and sidechain packing of the models provided by the Protein Health utility implemented in QUANTA (Molecular Simulations, 200 Fifth Avenue, Waltham, MA 02154, USA).
2. A quality factor furnished by the WHAT IF program [18], which assesses how normal or abnormal each sidechain environment is with respect to the average packing environment for all the residues of the same type in highly resolved Protein Data Bank structures.
3. Evaluation of the models against experimental structure/function data.

Results and discussion

The sequence alignment of the nAChR, GlyR, $GABA_A$R and 5-HT_3R subunit extracellular portions obtained with the CLUSTALW program [15] is shown in Fig. 1.

Comparative modelling efforts have been focused, up to now, on the derivation of three-dimensional models for the extracellular portion of the nAChR [10] and the GlyR [11]. The model of the nAChR extracellular domain [10] was derived using the sequence homology of the individual subunits with copper-binding protein of known crystal structure (plastocyanin and pseudoazurin), while the GlyR model [11] was based on a significant match with the SH2 and SH3 domains of the biotin repressor structure. For both models, conformance with a large number and variety of experimental data, such as site-specific mutagenesis, antibody mapping, and site-directed labelling studies, was checked; however, the two models proposed are indeed different.

The structural restraints imposed by the extracellular portion of the α, β, γ, and δ nAChR subunit models were exploited in the present work for the generation of the

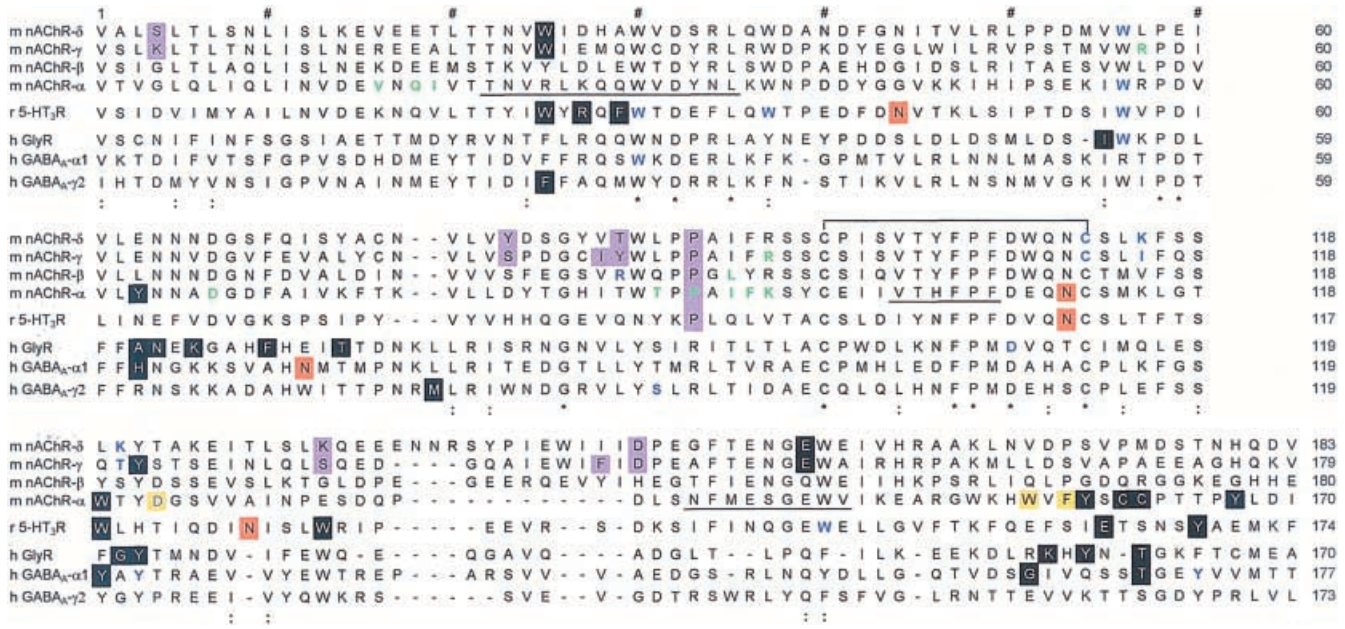

Fig. 1. Sequence alignment derived by CLUSTALW[15] of mouse nicotinic acetylcholine δ, γ, β and α receptor subunits (*nAChR*), rat 5-HT_3 receptor (*5-HT*$_3$R), human glycine receptor (*GlyR*), and human ψ-aminobutiric acid type A α1 and γ2 receptor subunits (*GABA*$_A$). Helical secondary structure elements derived from the template nAChR model [10] are *underlined*. Interesting residues are highlighted as follow: *red boxes* correspond to glycosylation sites, *yellow boxes* correspond to possible glycosylation sites upon mutation to form a glycosylation consensus signal, *reverse contrast* indicates residues putatively involved in ligand binding, *violet boxes* indicate residues involved in receptor conformational equilibrium, residues putatively involved in folding or receptor assembly are in *blue*, and residues forming possible membrane contact surfaces are reported in *green*

three-dimensional 5-HT_3R subunit structure by the program MODELLER [16]. The 5-HT_3R was then assembled on the pentameric arrangement of the template structure. The nAChR model was chosen as a template since it is the receptor most closely related to the 5-HT_3R in sequence (more than 30% similarity) and function (cation-selective LGICs mediate excitatory neurotransmission, whereas anion-selective LGICs are inhibitory).

3.1 Key residues for receptor structure and function

Compatibility of the 5-HT_3R model obtained with the experimental structural information available to date was checked. The most significant experimental results obtained by site-directed mutagenesis studies are summarized in Table 1. These provide intriguing, albeit not always consistent, clues about the structure/function of the member of the Cys-loop family of LGICs. The structural location of the mutated residues, which is also reported in Table 1, allows one to distinguish between the probable candidates for ligand interactions, subunit architecture and receptor assembly. Mutated residues, listed in Table 1, are reported in bold in the text.

The sidechains of **N44**, **N110** and **N126** are putative N-linked glycosylation sites**. N110** is the only N-linked glycosylation site conserved among the nAChR and 5-HT_3R subunits. Although its sidechain points towards the protein core, it is judged to be sufficiently solvent-accessible to support a surface oligosaccaride [10]. **N126** is exposed to the solvent in the pentamer model, while **N44** is buried and, according to recent experimental findings, it is not glycosilated [27]. A few charged residues (D14, K16, **R27** and R137) are found to be completely buried in the model. D14 and E134 form salt bridges with **R27** and R137, respectively, while K16 is neutralized by a charge-reinforced hydrogen bond with Ser112 and a salt bridge with D14. **R27** is located at the subunit interface and its mutation to alanine causes a detrimental effect on agonist binding [26]. According to our model this seems to be ascribed to a structural modification of the binding site.

Most of the totally or partially conserved residues in the Cys-loop class of LGICs are found in the core of the protein model, participating in the structural scaffold of the subunits. **W37** and **W149** lie on the protein surface; however, their importance in the determination of the tertiary structure of the 5-HT_3R subunit is confirmed by our three-dimensional model. In fact, **W37** is found to interact with the sidechain of **E148**, causing the stacking of loop 34–43 to the α helix formed by residues 142–150. Interestingly, mutation of residue **E148**, conserved in most of the nAChR subunits and otherwise represented by a glutamine residue, causes an effect on binding which, in the light of these observations, might be interpreted as a reflection of structural disturbance. **W25**, **W30**, **W56**, P58, D59, V79, G83 I101, F104 and P105 are in regions involved in intersubunit contacts and are expected to fulfil structural and assembly roles. Of these residues, **W25**, **W30** and **W56** have been mutated and good agreement is observed between the role postulated on the basis of the experimental findings and their

Table 1. Structural location and experimental responses of mutated residues in ligand-gated ion channel receptors

Residue	N (Fig. 1)	Receptor	Structural position	Experimental findings	Ref.
Ser36/Lys3	4	AChR-δ/γ	subunit interface (boundary)	Charge dependent conformational changes	19, 20
Trp55/Trp5′	25	AChR-γ/δ	subunit interface (core)	affects binding	19
Trp86	56	AChR-α/δ	subunit interface (boundary)	affects binding	19
Tyr93	63	AChR-α	subunit surface	affects binding	21
Ser111/Tyr′	81	AChR-γ/δ	subunit interface (core)	conformational equilibrium	21
Ile116	86	AChR-γ	subunit interface (core)	conformational equilibrium	21
Tyr117/Tyr′	87	AChR-γ/δ	subunit interface (boundary)	conformational equilibrium	21
Arg117	87	AChR-ß	subunit interface (boundary)	key role for surface expression	22
Pro121	91	AChR	subunit core	crucial for rapid opening of the channels	23
Asn141	111	AChR-α	exposed	glycosilation site	10
Ile145/Lys1	115	AChR-γ/δ	subunit surface	promotes subunit assembly	22
Trp149	119	AChR-α	subunit surface	affects binding	21, 24
Thr150/Lys	120	AChR-γ/δ	subunit surface	promotes subunit assembly	22
Tyr151	121	AChR-γ	subunit surface	affects binding	22
Asp152	122	AChR-α	subunit surface	counter charge/subunit assembly	20, 10
Ser161/Lys	131	AChR-γ/δ	subunit surface	conformational equilibrium/low affinity	21
Phe172	142	AChR-γ	subunit interface (boundary)	conformational equilibrium	21
Asp174/Asp	144/148	AChR-γ/δ	subunit interface (boundary)	conformational equilibrium	20
Trp187	156	AChR-α	subunit interface (boundary)	upon mutation to N, glycosylation occurs	10
Glu189	157	AChR-δ	subunit interface (boundary)	affects binding/subunit assembly	19
Phe189	158	AChR-α	subunit interface (boundary)	upon mutation to N, glycosylation occurs	10
Tyr190	159	AChR-α	subunit interface (boundary)	affects binding	21
Cys192	161	AChR-α	subunit interface (boundary)	affects binding	21
Cys193	162	AChR-α	subunit interface (boundary)	affects binding	21
Tyr198	167	AChR-α	subunit interface (core)	affects binding	21
Trp90	25	5-HT_3	subunit interface (core)	affects binding	25
Arg92	27	5-HT_3	subunit core	affects binding	26
Phe94	29	5-HT_3	subunit interface (core)	affects binding	26
Trp95	30	5-HT_3	subunit interface (core/boundary)	subunits assembly/folding	25
Trp102	37	5-HT_3	subunit surface	subunits assembly/folding	25
Asn109	44	5-HT_3	buried	not glycosilated	27
Trp121	56	5-HT_3	subunit interface (boundary)	subunits assembly/folding	25
Asn175	110	5-HT_3	exposed	glycosilation site	27
Trp183	118	5-HT_3	subunit surface	affects binding	25
Asn191	126	5-HT_3	exposed	glycosilation site	27
Trp195	130	5-HT_3	subunit surface	affects binding	25
Trp214	149	5-HT_3	subunit surface	subunits assembly/folding	25
Glu206	164	5-HT_3	subunit interface (boundary)	affects binding	28
Tyr234	169	5-HT_3	subunit interface (core)	affects binding	28
Phe77	25	$GABA_A$-γ2	subunit interface (core)	affects binding	29
Trp69	30	$GABA_A$-αl	subunit interface (core/boundary)	subunit assembly	30
Trp94	56	$GABA_A$-αl	subunit interface (boundary)	subunit assembly	30
His101	62	$GABA_A$-αl	subunit surface	affects binding	31
Asn110	71	$GABA_A$-αl	exposed	glycosilation site	30
Met130	78	$GABA_A$-γ2	subunit surface	affects binding	29
Ser142	90	$GABA_A$-γ2	subunit core	functional alteration	31
Tyr159	120	$GABA_A$-αl	subunit surface	affects binding/functional alteration	29
Tyr161	122	$GABA_A$-αl	subunit surface	functional alteration	31
Gly200	163	$GABA_A$-α1	subunit surface	affects binding	31
Thr206	169	$GABA_A$-αl	subunit interface (boundary)	affects binding/functional alteration	29
Tyr209	172	$GABA_A$-αl	subunit interface (core)	functional alteration	31
Ile93	54	GlyR	subunit interface (boundary)	affects binding	32
Trp94	55	GlyR	subunit interface (boundary)	subunit assembly	32
Ala101	62	GlyR	subunit surface	affects binding	32
Asn102	63	GlyR	subunit surface	affects binding	32
Lys104	65	GlyR	subunit surface	affects binding	33
Phe108	69	GlyR	subunit surface	affects binding	33
Thr112	73	GlyR	subunit surface	affects binding	33
Asp148	109	GlyR	subunit core	affects folding/assembly	34
Gly160	121	GlyR	subunt surface	affects binding	35
Tyr161	122	GlyR	subunit surface	affects binding	35
Lys200	158	GlyR	subunit interface (boundary)	affects binding	35
Tyr202	160	GlyR	subunit interface (boundary)	affects binding and receptor assembly	36
Thr204	162	GlyR	subunit interface (boundary)	affects binding	36

structural position in the model (Table 1). In fact, **W30** and **W56** are localized at the edge of the intersubunit crevice and might mediate subunit interactions in receptor assembly. **W25** lies in the core of the crevice and it is likely to have a key role in ligand binding, probably establishing a cation–π interaction with the protonated nitrogen present in the 5-HT_3R ligands [25]. It is worth noting that **W25** is conserved among the δ/γ nAChR and 5-HT_3R subunits and it is represented as a positively charged/polar residue in the α/β nAChR subunits, respectively. This might be the molecular determinant for the selectivity of the $\alpha\gamma$ and $\alpha\delta$ nAChR interfaces to form high-affinity binding sites for agonists and competitive antagonists.

In virtue of the three-dimensional model obtained, a structural role might be assumed for several mutated residues, which show impaired ligand binding in experiments carried out on the different members of this receptor family. In particular, residues **I115/K115**, **T120/K120** in the γ and δ nAChR chains and **D122** in the α nAChR chain are indeed indicated as subunit assembly promoters by experimental evidence [10, 22]. Their position on the protein surface in close proximity to the subunit interface suggests, at least for the δ subunit, a possible specific contribution to the electrostatic potential, which guides subunit assembly. Moreover, experimental evidence pointed out that **W118** is involved in ligand binding in both the 5-HT_3R [25] and the nAChR [24]. According to our model, **W118** is located on the surface at the far boundary of the intersubunit crevice; therefore, its direct involvement in ligand interaction has to be excluded. However, the region of amino acids between the 115–122 zone might be involved in intermolecular interactions with residues of the C-terminal 167–175, maintaining the binding site architecture.

Point mutations in the zone corresponding to loop 63–70 of the 5-HT_3R model were carried out on the anion-selective LGIC receptors and suggest the involvement of this stretch of amino acids in ligand binding. This hypothesis is not supported by our model; in fact it suggests that the amino acids in this region are likely to come in close apposition to the extracellular membrane face [10].

3.2 Key residues for receptor dynamics

Of particular interest is the **P90** residue, conserved in the cation-selective ion channels and shown to be involved in the rapid opening of the channel [23]. It is located at the end of a β strand that lies parallel to the α helix at the subunit interfaces (residues 20–30). Other residues participating at the same β strand (such as **Y81** and **T87** of the nAChR δ subunit and **S81**, **I86** and **Y87** of the nAChR γ subunit) have been shown to influence the conformational equilibrium of the receptor (Table 1). According to our 5-HT_3R model, **H80** (corresponding to **Y81** in the nAChR δ subunit) and E84 are located at the interface crevice and are possible candidate for ligand interactions.

It is worth noting that G83, whose strict conservation among the receptors of this family might suggest a possible active role in the mechanism of channel opening, lies in the same region,. Effects on the conformational equilibrium of the receptor have also been hypothesized for residues **S4**, **K131** and **D148** of the nAChR δ subunit and for residues **K4**, **S131**, **F142** and **D144** of the nAChR γ subunit [20, 21]. While the role of residues **K131** and **S131**, homologous to **W130** in the 5-HT_3R, is not obvious from the three-dimensional model obtained, an ionic intramolecular interaction that causes the packing of the N-terminal portion of the subunit chain with the remains of the protein is found in the three-dimensional model of the δ and γ nAChR subunits between residues **S4/K4** and **D144/D148**, respectively. An analogous interaction can be observed between residue **D4** and K140 of the 5-HT_3R.

3.3 Docking of ligands

Two hypotheses useful to guide the docking of ligands into the binding site were derived from a previous work, where quantitive structure activity relationship (QSAR) models were obtained for a wide series of newly synthesized ligands, designed to map systematically the receptor binding site. In fact, the results suggested that structurally different ligands might share a common binding domain and multiple modes of binding might be assumed for streoselective ligands.

On these bases, structurally different 5-HT_3R antagonists (arylpiperazine, quinuclidine and tropane derivatives) were superimposed and docked manually into the intersubunit crevice. Different orientations of the antagonists were tested and ligand–receptor interaction energies were used to classify the models and select the one shown in Fig. 2. Such a model suggests the antagonist binding site to be formed by residues **I55**, F104, F158, **Y169** and **E171** of the first subunit (analogous to subunit α1 in the nAChR model) [10] and **W25** in the second subunit (analogous to subunit γ in the nAChR model). Therefore, correspondences with the pharmacophoric hypothesis previously derived can be summarized as follows:

1. A charge-assisted hydrogen-bonding interaction can occur between the positively charged head of the antagonist and the negatively charged carboxylic tail of **E171**; this interaction is enhanced by the spatial proximity of **W25**.
2. A hydrogen-bonding interaction between the nitrogen ligand or the oxygen atom and **Y169**.
3. A specific interaction between the ligand aromatic moiety and F104 and/or F158.
4. Short-range dispersion interactions can be accomplished between ligand substituents and **I55**.

Among the residues involved in the antagonist binding some were mutated in members of the LIGC family. In particular, the residue corresponding to **E171** (**Y167** in the nAChR α subunit, Table 1, Fig. 1) has been suggested to interact directly with ammonium in the nAChR, **Y169** has been reported to be a key residue for ligand binding in the 5-HT_3R, and for **I55** a structural role in the GlyR subunit assembly has been reported.

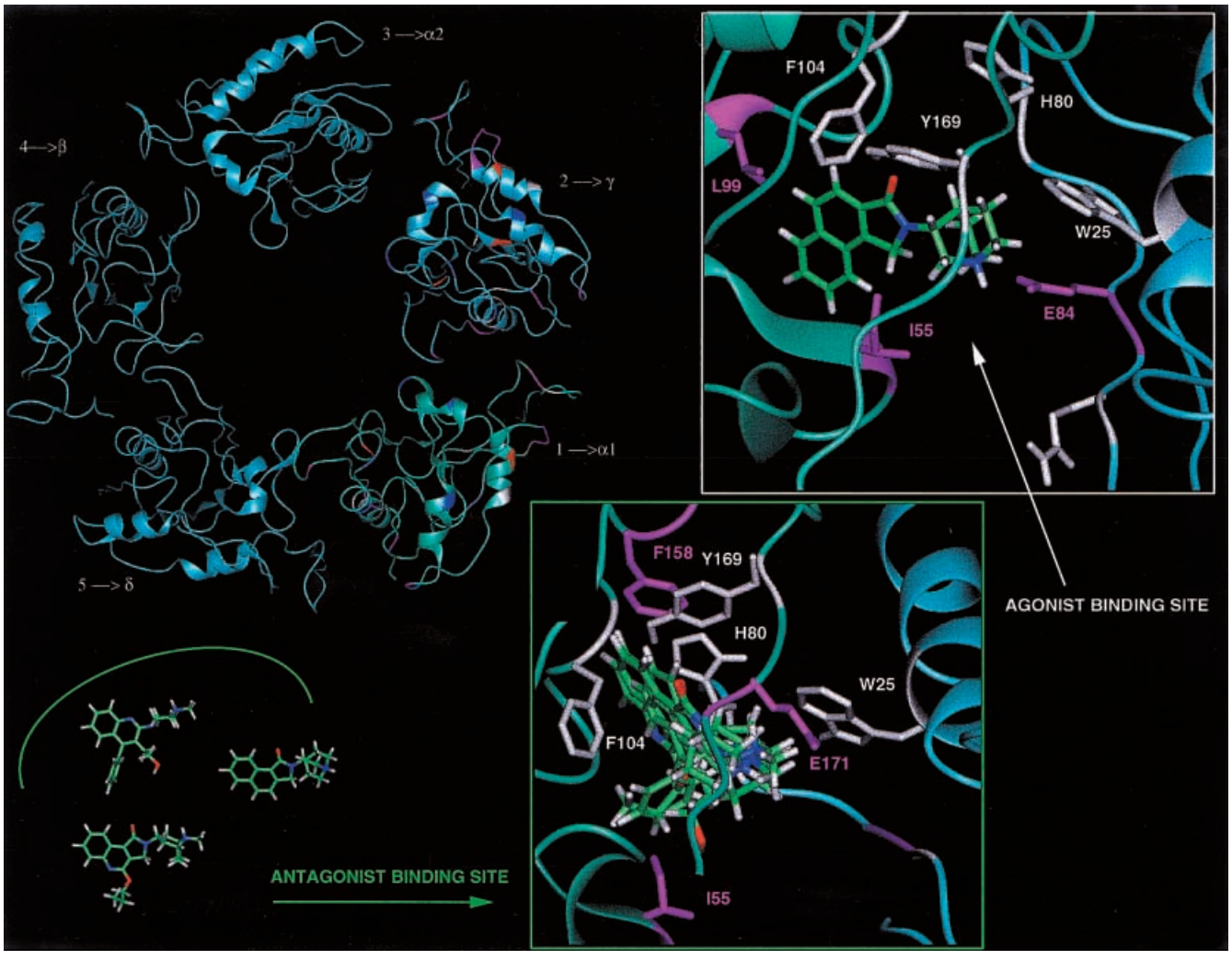

Fig. 2. Representation of the 5-HT_3R extracellular domain model; correspondence with the nAChR heterosubunits is indicated (*top left*). Tentative binding sites for agonists (*top right*) and antagonists (*bottom right*). The molecular structure of the ligands which constitute the supermolecule chosen to illustrate the antagonist binding site are shown. Only side chains of the residues implicated in ligand binding are shown and are coloured *white* if mutations are reported in one of the ligand-gated ion channel receptors or *violet* if no experimental information is available

Different binding modalities are hypothesized for the quinuclidine derivative with potent agonist activity (Fig. 2). Functional studies revealed a marked stereoselectivity of this ligand; in fact, the R enantiomer shows strong agonist behaviour, while the S enantiomer is a potent antagonist. It is worth stressing that also the quinuclidine derivative docked in the antagonist binding site proved to be an antagonist or a partial agonist depending on its S or R enantiomeric form.

According to the model, the main interaction of the agonist is achieved with E84. A negatively charged residue in this position is a peculiarity of the 5-HT_3R (Fig. 1). The residue is located, together with **H80**, in a β strand constituted by amino acids that regulate the receptor conformational equilibrium and leading to **P90**, the cardinal residue for receptor function. Also in this case, the ionic interaction is accompanied by a π-charge interaction with **W25**. The remains of the agonist binding site overlap with that of the antagonist, and the correspondences with the pharmacophoric model for receptor binding are corroborated.

The hypothesis of two distinct but overlapping binding sites is tempting since it constitutes a simple answer to the key question of what is the characteristic structural feature explaining the functional difference between agonists and competitive antagonists. However, it can only be substantiated by further experimental investigations. Alternative hypotheses are suggested by the model obtained and have to be verified by a comparative molecular dynamics analysis of a wide series of ligands, with full range of intrinsic affinities. In particular, the mutual positions of the two negatively charged residues involved in electrostatic interactions with the agonists and the antagonists and the topography of the interface crevice suggest that, in a dynamic view, the cationic head of the ligands might provide the origin for a sort of transiently concomitant resonant interaction with the two glutamate residues and that other molecular

determinants might be responsible for the activation/deactivation of the receptor.

4 Conclusions

The results of extensive checks on the consistency of the 5-HT_3R extracellular domain model with the experimental information available to date were satisfactory. Therefore, the choice of the recently published nAChR model to be used as a template is corroborated, although a few observed incongruities suggest that the modelling of a very localized region of the receptor could be ameliorated.

The analysis of the three-dimensional model allows one to distinguish among amino acids that exert key roles in ligand interactions, subunit architecture, receptor assembly and receptor dynamics. For some of these, alternative roles with respect to the one hypothesized by experimentalists are assigned. In this regard, it is worth stressing that conclusions based on mutations and functional assays alone might sometimes be ambiguous and the insights derived by the structural model obtained in this study can be exploited to suggest directions for experimental investigations.

In particular, regulation of ligand binding by structural changes that affect the interface of the subunits has been largely explored, from an experimental point of view, but the exact roles of the various residues in stabilizing the binding of agonists and in transmitting conformational changes to the ion channel are nonetheless poorly defined.

Two distinct but overlapping binding sites for agonists and competitive antagonists are proposed here on the basis of the correspondences between the topography of the amino acids putatively involved in ligand binding and the pharmacophore hypothesis derived by previously obtained QSAR models. It is proposed that the binding modalities of the agonists and anatgonists differ mainly for the negatively charged amino acid chosen as counterions. Competitive antagonists bind preferentially to E171 in the first subunit (corresponding to subunit $\alpha 1$ in the nAChR model), while agonists interact with E84 in the second subunit (corresponding to subunit γ in the nAChR model). E84 is part of a chain of amino acids that regulates the receptor conformational equilibrium and culminates in P90, the crucial residue for rapid opening of the channel. Alternative hypotheses can be derived from the analysis of ligand–receptor dynamics; however, the extent to which the conjectures made from the model are consistent will become apparent only once additional experimental data is available.

Acknowledgements. Thanks are due to MURST (ex40% and ex60% funds) and CNR for financial support.

References

1. Karlin A, Akabas MH (1995) Neuron 15: 1231–1244, and references therein
2. Unwin N (1993) J Mol Biol 229: 1101–1124
3. Corringer P-J, Le Novere N, Changeux J-P (2000) Annu Rev Pharmacol Toxicol 40: 431–458
4. Eisele JL, Bertrand S, Galzi JL, Devillers-Thiery A, Changeux J-P, Bertrand D (1993) Nature 366: 469–492
5. Jackson MB, Yakel JL (1995) Annu Rev Physiol 57: 447–468
6. Davies PA, Pistis M, Hanna MC, Peters JA, Lambert JJ, Hales TG, Kirkness EF (1999) Nature 397: 259–363
7. Wohland T, Friedrich K, Hovius R, Vogel H (1999) Biochemistry 38: 8671–8681
8. Le Novere N, Corringer PJ, Changeux J-P (1999) Biophys J 76: 2329–2345
9. Ortella MO (1997) Proteins 29: 391–398
10. Tsigenly I, Sugiyama N, Sine SM, Taylor P (1997) Biophys J 73: 52–56
11. Gready JE, Ranganathan S, Schofield PR, Matsuo T, Nishikawa K (1997) Protein Sci 6: 983–998
12. Cappelli A, Donati A, Anzini M, Vomero S, De Benedetti PG, Menziani MC, Langer T (1996) Bioorg Med Chem 4: 1255–1269
13. Cappelli A, Anzini M, Vomero S, Mennuni L, Makovec F, Doucet E, Hamon M, Bruni G, Romeo MR, Menziani MC, De Benedetti PG, Langer T (1998) J Med Chem 41: 728–741
14. Cappelli A, Anzini M, Vomero S, Canullo L, Mennuni L, Makovec F, Doucet E, Hamon M, Menziani MC, De Benedetti PG, Bruni G, Romeo MR, Giorgi G, Donati A (1999) J Med Chem 42: 1556–1575
15. Thompson JD, Higgins DG, Gibson TJ (1994) Nucleic Acids Res 22: 4673–4680
16. Sali A, Blundell TL (1993) J Mol Biol 234: 779–815
17. Brooks BR, Bruccoleri RE, Olafson BD, States DJ, Swaminathan S, Karplus M (1983) J Comput Chem 4: 187–217
18. Vriend G (1990) J Mol Graphics 8: 52–56
19. Hucho F, Tseltlin VI, Machold J (1996) Eur J Biochem 239: 539–557
20. Song X-Z, Pedersen SE (2000) Biophys J 78: 1324–1334
21. Papineni RVL, Pedersen E (1997) J Biol Chem 272: 24891–24898
22. Kreienkamp H-J, Maeda RK, Sine SM, Taylor P (1995) Neuron 14: 635–644
23. Ohno K, Wang HL, Milone M, Bren N, Brengman J, Nakano S, Quiram P, Pruitt J, Sine SM, Engel A (1996) Neuron 17: 157–170
24. Zhong W, Gallivan JP, Zhang Y, Li L, Lester HA, Dougherty DA (1998) Proc Natl Acad Sci USA 21: 12088–12093
25. Spier AD, Lummis SCR (2000) J Biol Chem 275: 5620–5625
26. Yan D, Schulte MK, Bloom KE, White MM (1999) J Biol Chem 274: 5537–5541
27. Fletcher E, Sepulveda MI, Green T, Pinnock R, Lummis SCR (1995) Neurosci Abstr 21: 343
28. Hope AG, Belelli D, Mair ID, Lambert JJ, Peters JA (1999) Mol Pharmacol 55: 1037–1043
29. Sigel E, Schaerer MT, Buhr A, Baur R (1998) Mol Pharmacol 54: 1097–1105
30. Srinivasan S, Nichols CJ, Lawless GM, Olsen RW, Tobin AJ (1999) J Biol Chem 274: 26633–26638
31. Sigel E, Buhr A (1997) Trends Pharmacol Sci 18: 425–429
32. Vafa B, Lewis TM, Cunnigham AM, Jacques P, Lynch JW, Schofield PR (1999) J Neurochem 73: 2158–2166
33. Schmieden V, Kuhse J, Betz H (1999) Mol Pharmacol 56: 464–472
34. Vandenberg RJ, Rajendra S, French CR, Barry PH, Schofield PR (1993) Mol Pharmacol 44: 198–203
35. Vandenberg RJ, French CR, Barry PH, Schine J, Schofield PR (1992) Proc Natl Acad Sci USA 89: 1765–1769
36. Rajendra S, Vandenberg RJ, Pierce KD, Cunnigham AM, French PW, Barry PH, Schofield PR (1995) EMBO J 14: 2987–2998